Quantum-coherence-enhanced transient surface plasmon lasing

2017 J. Opt. 19 054002

(http://iopscience.iop.org/2040-8986/19/5/054002)

IOP Publishing Journal of Optics
J. Opt. 19 (2017) 054002 (6pp) https://doi.org/10.1088/2040-8986/aa6097

Quantum-coherence-enhanced transient surface plasmon lasing

Pankaj K Jha[1], Yuan Wang[1], Xuexin Ren[1] and Xiang Zhang[1,2,3]

[1] NSF Nanoscale Science and Engineering Center (NSEC), 3112 Etcheverry Hall, University of California, Berkeley, California 94720, United States of America
[2] Materials Science Division, Lawrence Berkeley National Laboratory, 1 Cyclotron Road Berkeley, California 94720, United States of America

E-mail: xiang@berkeley.edu

Received 13 June 2016, revised 8 December 2016
Accepted for publication 15 February 2017
Published 23 March 2017

Abstract

Quantum coherence and interference offer novel pathways to control light–matter interaction at the atomic scale, with enticing prospects in both fundamental and applied science. Here, we demonstrate coherent control over transient excitation of localized surface plasmon modes of a silver nanosphere adjacent to a quantum coherence medium composed of three-level quantum emitters, using a theoretical approach. We show that quantum interference enables more than two orders of magnitude enhancement in the surface plasmon field generated when the quantum emitters are driven coherently, in comparison to incoherent pumping. Furthermore, under optimal conditions, intense surface plasmon lasing can be induced without population inversion on the spasing transition. Our results open up the possibility of overcoming dissipative losses in plasmonic modes in the transient regime when steady-state population inversion is difficult to achieve due to fast relaxation rates and impractical pumping requirements.

Keywords: quantum coherence, spaser, lasing

(Some figures may appear in colour only in the online journal)

Quantum engineering of light–matter interactions is an active field of research with far-reaching applications ranging from physics, chemistry and materials science to nanotechnology [1–3]. In the past decade confining light to nanoscale environments via coupling to the conduction electrons of metal nanostructures has led to several significant applications in microscopy, single-molecule detection, sensing and optical circuits [4–9]. In particular, spaser (surface plasmon amplification by stimulated emission of radiation) technology has attracted monumental interest owing to its enticing prospect of using coherent fields at the nanoscale [10–12]. However, quantum optical application down to the single photon-level [13] is still an outstanding challenge owing to the inherent absorption loss in the metal. Presence of an optical gain can be used to mitigate loss [14–23]. However, the gain provided by active medium is not always sufficient, particularly in the shorter wavelengths, for e.g. the ultra-violet (UV) regime, due to impractical pumping requirements [24–26].

On the other hand, quantum coherence and interference in multi-level quantum emitters has led to several outstanding effects in physics for e.g. electromagnetic induced transparency (EIT) [27, 28], lasing without inversion (LWI) [29][4], ultraslow light [30, 31], ultrasensitive magnetometry [32] and high resolution nonlinear spectroscopy [33, 34]. Recently, it has been proposed that quantum coherence can be harnessed to create quantum metamaterials with exotic properties not readily found in nature [35]. Experimental and theoretical investigations have provided strong evidence that quantum coherence also plays crucial roles where the system strongly interacts with the dissipative environment, for instance, in biological systems [36, 37].

[3] Author to whom any correspondence should be addressed.

[4] See [29] for review articles on LWI theory and concepts.

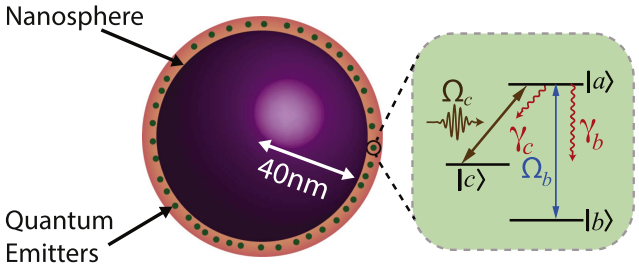

Figure 1. A silver nanosphere of radius $r = 40$ nm embedded in a homogeneous dielectric exhibiting optical gain. The level structure of the gain medium as three-level (Λ-configuration) quantum emitters is shown in the inset box. In contrast to two-level, three-level quantum emitters benefit from the possibility to coherently tailor their optical response using external fields (for e.g. Ω_c). To explore the transient regime, the gain medium is excited to states $|a\rangle$ and $|c\rangle$ by a flash; however, after a short time $t \ll \gamma_b^{-1}$, a strong coherent field is applied to drive the transition $|a\rangle \leftrightarrow |c\rangle$. The quantum emitter goes to the ground state $|a\rangle \rightarrow |b\rangle$ by exciting the dipolar plasmonic mode of the nanosphere.

In this work we demonstrate, theoretically, the possibility of harnessing quantum coherence in a multi-level quantum emitter based gain medium, excited by external fields, to control and manipulate the generation of localized surface plasmons in the transient regime. Crucially, we show that quantum coherence enables two orders of magnitude enhancement in the plasmon field, in comparison to incoherent drive, by mitigating surface plasmon absorption. We show stronger emission of surface plasmons without population inversion on the spasing (surface plasmon analog of lasing) transition—analogous to LWI. Our results open the door for creating gain and overcoming the dissipative plasmonic modes even when steady-state population inversion is difficult to achieve due to fast relaxation rates and impractical pumping requirements.

Our system, depicted in figure 1, consists of a silver nanosphere embedded in a homogeneous dielectric exhibiting optical gain. We have modeled the gain medium as a generic three-level quantum emitter in Λ-configuration, where the transitions $|a\rangle \leftrightarrow |b\rangle$ and $|a\rangle \leftrightarrow |c\rangle$ are dipole allowed while the transition $|c\rangle \leftrightarrow |b\rangle$ is dipole forbidden. The transition $|a\rangle \leftrightarrow |c\rangle$ is driven by an external coherent field of Rabi frequency Ω_c. It is advantageous to use multi-level quantum emitters, excited by external coherent fields, to control and manipulate surface plasmons on meta-dielectric interfaces or localized on metallic structures with dimensions of the order of or smaller than wavelengths. In contrast to two-level, three-level quantum emitters benefit from the possibility to coherently tailor their optical response using external fields and also quantum vacuum [38, 39]. To neglect any deleterious effects caused by direct excitation of the spasing transition by the coherent drive field Ω_c, we have assumed the resonant frequency ω_{ac} to differ significantly from the frequency ω_{ab} for e.g. $|a\rangle \rightarrow |b\rangle$ corresponding to UV while $|a\rangle \rightarrow |c\rangle$ lies in the near infra-red (NIR) regime.

We employ semiclassical theory to study the light–matter interaction. We treat the gain medium quantum mechanically and the localized plasmons and the photons classically [40–42]. We consider the plasmon and photon field $a_n(t) = \alpha_n(t)\exp[-\mathrm{i}\omega_s]t$, $b_n(t) = \beta_n(t)\exp[-\mathrm{i}\omega_c]t$ where $\alpha_n(t)$ and $\beta_n(t)$ are slowly varying amplitudes. The number of localized surface plasmons per mode is $\mathcal{N}_n(t) = |\alpha_n(t)|^2$. The interaction Hamiltonian can be written as

$$\mathcal{V} = -\sum_j (\hbar\Omega_b^{(j)} \mathrm{e}^{\mathrm{i}\Delta_b t}|a\rangle\langle b| + \hbar\Omega_c^{(j)}\mathrm{e}^{\mathrm{i}\Delta_c t}|a\rangle\langle c| + \mathrm{h.c.}) \quad (1)$$

where $\Omega_b^{(j)} = -A_n\vec{\wp}_{ab}^{(j)}\cdot\vec{\nabla}\varphi(\vec{r}_j)\alpha_n/\hbar = \Omega^{(j)}\alpha_n$ is the Rabi frequency for the spasing transition $|a\rangle \rightarrow |b\rangle$ while $\Omega_c^{(j)} = \vec{\wp}_{ac}^{(j)}\cdot\vec{E}_c(\vec{r}_j)\beta_n/\hbar$ is the Rabi frequency for the driven transition $|a\rangle \leftrightarrow |c\rangle$. Here the summation is over all the *jth* quantum emitters and we define the detunings as $\Delta_b = \omega_{ab} - \omega_b$ and $\Delta_c = \omega_{ac} - \omega_c$. The master equation for the quantum emitter density matrix ρ is of the Lindblad form

$$\frac{\mathrm{d}\rho}{\mathrm{d}t} = -\frac{\mathrm{i}}{\hbar}[\mathcal{V}, \rho] - \mathcal{L}\rho \quad (2)$$

where $\mathcal{L}$ is the Lindblad superoperator which quantifies the dissipative part of the master equation. The three-level quantum emitter shown in figure 1 the dissipative part is given by

$$\mathcal{L}\rho = \frac{\gamma_b}{2}(\sigma_b^\dagger\sigma_b\rho + \rho\sigma_b^\dagger\sigma_b - 2\sigma_b\rho\sigma_b^\dagger) + \frac{\gamma_c}{2}(\sigma_c^\dagger\sigma_c\rho + \rho\sigma_c^\dagger\sigma_c - 2\sigma_c\rho\sigma_c^\dagger) \quad (3)$$

in which $\sigma_c = |c\rangle\langle a|$, $\sigma_b = |b\rangle\langle a|$, $\sigma_c^\dagger = |a\rangle\langle c|$, $\sigma_b^\dagger = |b\rangle\langle a|$, γ is the spontaneous decay rate on the corresponding transitions. To eliminate the fast oscillating exponentials we use the following transformation

$$\rho_{ab} = \varrho_{ab}\mathrm{e}^{\mathrm{i}\Delta_b t},\ \rho_{ac} = \varrho_{ac}\mathrm{e}^{\mathrm{i}\Delta_c t},\ \rho_{cb} = \varrho_{cb}\mathrm{e}^{\mathrm{i}(\Delta_b-\Delta_c)t}. \quad (4)$$

From equations (1)–(3) the density matrix equations can be written as

$$\dot{\varrho}_{ab} = -\Gamma_{ab}\varrho_{ab} - \mathrm{i}\Omega\alpha_n(\varrho_{aa} - \varrho_{bb}) + \mathrm{i}\Omega_c\varrho_{cb}, \quad (5)$$

$$\dot{\varrho}_{cb} = -\Gamma_{cb}\varrho_{cb} + \mathrm{i}\Omega_c^*\varrho_{ab} - \mathrm{i}\Omega\alpha_n\varrho_{ca}, \quad (6)$$

$$\dot{\varrho}_{ca} = -\Gamma_{ca}\varrho_{ca} + \mathrm{i}\Omega_c^*(\varrho_{aa} - \varrho_{cc}) - \mathrm{i}\Omega^*\alpha_n^*\varrho_{cb}. \quad (7)$$

Equations (4)–(9) are supplemented by their complex conjugates. The evolution of the population terms are given by

$$\dot{\varrho}_{bb} = \gamma_b\varrho_{aa} + \mathrm{i}(\Omega^*\alpha_n^*\varrho_{ab} - \Omega\alpha_n\varrho_{ab}^*), \quad (8)$$

$$\dot{\varrho}_{cc} = \gamma_c\varrho_{aa} + \mathrm{i}(\Omega_c^*\varrho_{ac} - \Omega_c\varrho_{ac}^*). \quad (9)$$

The population conservation requires $\sum\varrho_{ii} = 1$. The off-diagonal relaxation rates are given as $\Gamma_{ab} = \gamma_{ab} + \mathrm{i}\Delta_b$, $\Gamma_{ac} = \gamma_{ac} + \mathrm{i}\Delta_c$, $\Gamma_{cb} = \gamma_{cb} + \mathrm{i}(\Delta_b - \Delta_c)$. Here $\gamma_{ab} = (\gamma_b + \gamma_c)/2$, $\gamma_{ac} = (\gamma_b + \gamma_c)/2$, $\gamma_{cb} = 0$. The evolution of the plasmon field is obtained by the Heisenberg equation of motion for the amplitude α_n

$$\dot{\alpha}_n = -\Gamma_n\alpha_n + \mathrm{i}\sum_j \Omega^{*(j)}\varrho_{ab}^{(j)} \quad (10)$$

where $\Gamma_n = \gamma_n + \mathrm{i}\Delta_n$, $\Omega^{(j)} = -A_n\vec{\wp}_{ab}^{(j)}\cdot\vec{\nabla}\varphi(\vec{r}_j)/\hbar$. Next we assume that the Rabi frequencies for all the quantum emitters are the same, i.e. $\sum_j \rightarrow \mathcal{N}$ where $\mathcal{N}$ is the total number of quantum emitters. For numerical calculation we have

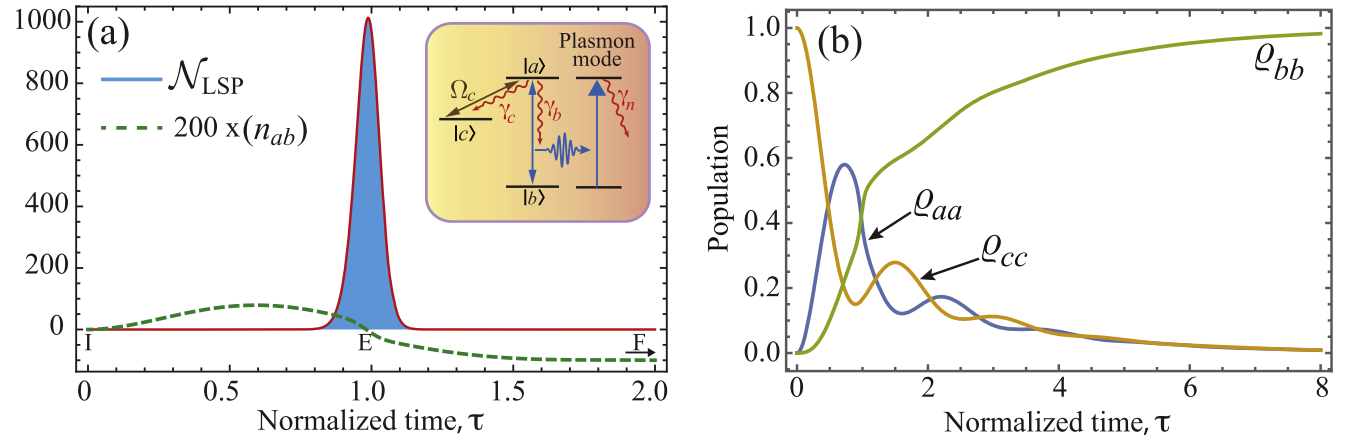

Figure 2. (a) Plot of the number of localized surface plasmons (solid curve) and scaled inversion between the states $|a\rangle$ and $|b\rangle$ (dashed curve) versus normalized time $\tau = \gamma_b t$ for the initial condition $\varrho_{cc}(0) = 1.0$, $\varrho_{aa}(0) = \varrho_{bb}(0) = 0$. An intense surface plasmon pulse generated when the quantum emitter decays to the ground state $|b\rangle$. The inset shows the three-level quantum emitter in Λ-configuration initially prepared in the excited state $|c\rangle$. When the emitter is coherently driven to state $|a\rangle$ it decays to the ground state $|b\rangle$ by emitting a surface plasmon. The local field of SPs provides feedback by stimulating the $|a\rangle \rightarrow |b\rangle$ transition. (b) Temporal evolution of population (ϱ_{xx}) of the state $|x\rangle$. For numerical simulation we considered dipolar LSP mode of a silver nanosphere and surrounded by a dielectric medium of permittivity $\epsilon_{\rm d} = 2.25$. The number density of the quantum emitter is $\mathcal{N} = 0.92 \times 10^{21}\,{\rm cm}^{-3}$ and the Rabi frequency of the drive field $\Omega_c = 2.0$.

assumed resonant interaction between the quantum emitters and the localized surface plasmon mode of the silver nanosphere. Under this assumption and the weak plasmon field, the off-diagonal term ϱ_{ab} is purely imaginary. Writing $\varrho_{ab} = {\rm i}\Omega\alpha_n\sigma_{ab}$ where α_n is real yields σ_{ab} as real. Now from equation (10) we obtain

$$\dot{\alpha}_n = -(\Gamma_n + \mathcal{M}|\Omega|^2\sigma_{ab})\alpha_n. \tag{11}$$

From equation (8) we can write (assuming Ω, α_n are real)

$$\sigma_{ab} = \frac{\gamma_b\varrho_{aa} - \dot{\varrho}_{bb}}{2\Omega^2\alpha_n}. \tag{12}$$

From equation (11), the amplification of LSP requires $\sigma_{ab} < 0$ which implies $\gamma_b\varrho_{aa} < \dot{\varrho}_{bb}$. In steady-state $\dot{\varrho}_{bb} = 0$ and subsequently $\sigma_{ab} > 0$, which yields no amplification. However in the transient regime it is possible to achieve amplification [43–46].

Now we present numerical simulation results obtained by solving equations (3)–(8). We consider the lower transition $|a\rangle \rightarrow |b\rangle$ of the quantum emitter is resonantly coupled with the dipolar localized surface plasmon (LSP) mode of a silver nanosphere. The nanosphere is surrounded by a homogeneous dielectric of permittivity $\epsilon_d = 2.25$. We considered a silver nanosphere of 40 nm radius and the corresponding surface plasmon resonance at $\hbar\omega_n \sim 2.5$ eV and the decay rate $\gamma_n \sim 10^{14}\,{\rm s}^{-1}$ [47]. The decay rates of the quantum emitters are $\gamma_b = 4 \times 10^{12}\,{\rm s}^{-1}$, $\gamma_c = 2.8 \times 10^{11}\,{\rm s}^{-1}$ and the dipole moment $\wp_{ab} \sim ea_0$, where a_0 is the Bohr radius.

We begin with the scenario where the quantum emitters have been prepared in the excited state $|c\rangle$. This corresponds to the maximum Raman inversion (defined as $\varrho_{aa} + \varrho_{cc} - \varrho_{bb}$) for a three-level quantum emitter. Next we drive the transition $|a\rangle \leftrightarrow |c\rangle$ by a coherent drive field Ω_c. The coherent drive in such Λ-configuration induce quantum interference among the excitation channels and yield asymmetry in emission and absorption rates [48]. This lies at the heart of LWI and related effects [49]. In figure 2(a) we have plotted the temporal evolution of the localized surface plasmon $\mathcal{N}_{\rm LSP}(\tau) = |\alpha_n(\tau)|^2$. We see an intense pulse of localized surface plasmon generated around time $t \sim \gamma_b^{-1}$. The total number of LSPs, defined as $\mathcal{N}_{\rm LSP}^{\rm Int} = \int_0^\infty \mathcal{N}_{\rm LSP}(\tau){\rm d}\tau$, in the pulse is ≅110. In figure 2(b) we have plotted the temporal evolution of population of the states $|a\rangle$, $|b\rangle$ and $|c\rangle$. We see that the oscillations in the populations of levels $|a\rangle$ and $|c\rangle$ are prominent and after a few oscillations the quantum emitter decays to the ground state $|b\rangle$. The surface plasmon peak emission occurs at $\varrho_{aa} = \varrho_{bb} \sim 0.4$, and the population of level $|c\rangle$ is $\varrho_{cc} \sim 0.2$.

Quantum interference is very fragile, and severely affected by decoherence due to coupling with the environment; as such, it may seem that extending coherence effects to plasmonics may not survive owing to ultrafast relaxation time scale of the surface plasmons (SP) and large intrinsic losses. To illustrate the role of atomic coherence, we consider the initial condition $\varrho_{aa}(0) = 1$, $\varrho_{cc}(0) = \varrho_{bb}(0) = 0$ with a coherent drive field on the transition $|a\rangle \leftrightarrow |c\rangle$. Similar for figure 2(a), the system begins to spase with population inversion $\varrho_{aa} > \varrho_{bb}$ (as shown by blue shaded region in figure 3(a)), however, after short time, a much stronger plasmon pulse is emitted without population inversion $\varrho_{aa} < \varrho_{bb}$ (as shown by purple shaded region in figure 3(a)). However, the total population inversion is defined as $\varrho_{cc} + \varrho_{cc} - \varrho_{bb} > 0$. The total number of LSP in the presence of the drive is $\mathcal{N}_{\rm LSP}^{\rm Int} \cong 300$ where the ratio of LSPs with and without population inversion is 1:5. Next, we start with the same initial condition, but now replace the coherent drive with an incoherent pump which drives the transiton $|a\rangle \leftrightarrow |c\rangle$ at a rate $\mathcal{R}$. The interaction Hamiltonian can be

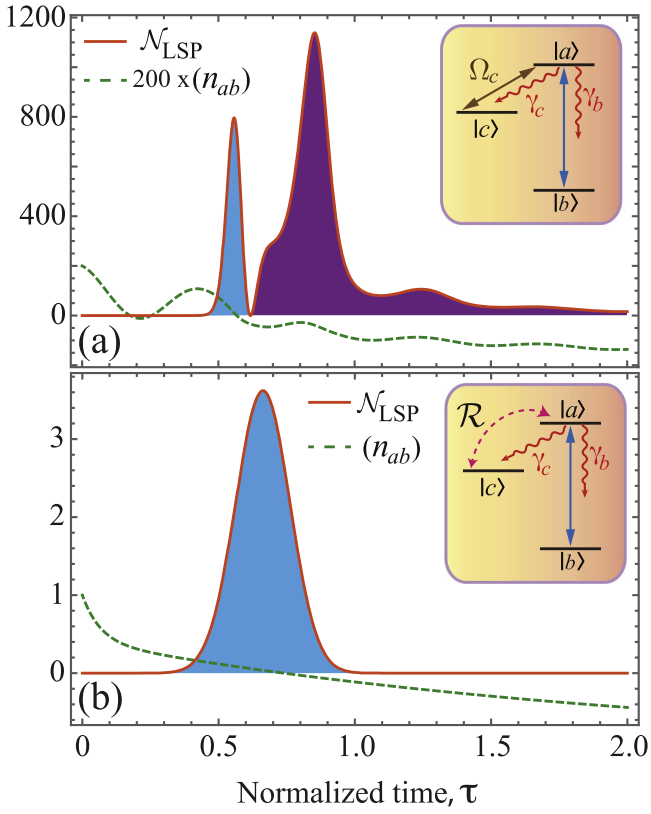

Figure 3. Plot of the number of localized surface plasmons (solid curve) and scaled inversion between the states $|a\rangle$ and $|b\rangle$ (dashed curve) versus normalized time $\tau = \gamma_b t$ for the initial condition $\varrho_{aa}(0) = 1$, $\varrho_{cc}(0) = \varrho_{bb}(0) = 0$. (a) We apply a coherent drive field of Rabi frequency $\Omega_c = 6.9\gamma_b$. (b) We apply an incoherent bidirectional pump $\mathcal{R} = 6.9\gamma_b$. In both scenarios, the system starts to lase with population inversion $n_{ab} > 0$ (as shown by blue shaded region in (a, b)). However, with coherent field Ω_c building up and strengthening the Raman coherence ϱ_{cb}, a much stronger plasmon pulse is emitted without population inversion $n_{ab} < 0$ (as shown by purple shaded region in (a)). Subsequently, with coherent drive the total number of LSP generated $\mathcal{N}_{\rm LSP}^{\rm Int}$ is more than two orders of magnitude higher compared to bidirectional incoherent pumping under the same conditions. The number density of the quantum emitter is $\mathcal{N} = 1 \times 10^{21}\,{\rm cm}^{-3}$.

written as

$$\mathcal{V}_{\rm I} = -\sum_j (\hbar\Omega_b^{(j)} e^{i\Delta_b t}|a\rangle\langle b| + {\rm h.c.}) \tag{13}$$

where $\Omega_b^{(j)} = -A_n \vec{\wp}_{ab}^{(j)} \cdot \vec{\nabla}\varphi(\vec{r}_j)\alpha_n/\hbar = \Omega^{(j)}\alpha_n$ is the Rabi frequency for the spasing transition $|a\rangle \rightarrow |b\rangle$. The master equation for the quantum emitter density matrix ρ is of the Lindblad form given by equation (2) with $\mathcal{V}$ replaced by $\mathcal{V}_{\rm I}$. In the presence of the incoherent pump $\mathcal{R}$, the dissipative part of the master equation takes the form

$$\begin{aligned}\mathcal{L}\rho = {}& \frac{\gamma_b}{2}(\sigma_b^\dagger\sigma_b\rho + \rho\sigma_b^\dagger\sigma_b - 2\sigma_b\rho\sigma_b^\dagger) \\ & + \frac{\gamma_c + \mathcal{R}}{2}(\sigma_c^\dagger\sigma_c\rho + \rho\sigma_c^\dagger\sigma_c - 2\sigma_c\rho\sigma_c^\dagger) \\ & + \frac{\mathcal{R}}{2}(\sigma_c\sigma_c^\dagger\rho + \rho\sigma_c\sigma_c^\dagger - 2\sigma_c^\dagger\rho\sigma_c).\end{aligned} \tag{14}$$

To eliminate the fast oscillating exponentials we use the following transformation: $\rho_{ab} = \varrho_{ab}e^{i\Delta_b t}$, $\rho_{cb} = \varrho_{cb}e^{i\Delta_b t}$. From equations (1)–(3) the density matrix equations can be written as

$$\dot{\varrho}_{ab} = -\Gamma_{ab}\varrho_{ab} - i\Omega\alpha_n(\varrho_{aa} - \varrho_{bb}), \tag{15}$$

$$\dot{\varrho}_{cb} = -\Gamma_{cb}\varrho_{cb} - i\Omega\alpha_n\varrho_{ca}, \tag{16}$$

$$\dot{\varrho}_{ca} = -\Gamma_{ca}\varrho_{ca} - i\Omega^*\alpha_n^*\varrho_{cb}. \tag{17}$$

Equations (15)–(17) are supplemented by their complex conjugates. The evolution of the population terms are given by

$$\dot{\varrho}_{bb} = \gamma_b\varrho_{aa} + i(\Omega^*\alpha_n^*\varrho_{ab} - \Omega\alpha_n\varrho_{ab}^*), \tag{18}$$

$$\dot{\varrho}_{cc} = (\gamma_c + \mathcal{R})\varrho_{aa} - \mathcal{R}\varrho_{cc}. \tag{19}$$

Population conservation requires $\sum\varrho_{ii} = 1$. The off-diagonal relaxation rates are given as $\Gamma_{ab} = \gamma_{ab} + i\Delta_b$, $\Gamma_{ac} = \gamma_{ac} + i\Delta_c$, $\Gamma_{cb} = \gamma_{cb} + i(\Delta_b - \Delta_c)$. Here $\gamma_{ab} = (\gamma_b + \gamma_c + \mathcal{R})/2$, $\gamma_{ac} = (\gamma_b + \gamma_c + 2\mathcal{R})/2$, $\gamma_{cb} = \mathcal{R}/2$. Next we solve for the amplitude of the plasmon field α_n and the result is shown in figure 3(b). Here, the system begin to spase with population inversion only. However, the surface plasmon field is more than two orders of magnitude weaker than the case with coherent drive excitation. From equation (5) we see that the quantum coherence and interference is captured by the Raman coherent term ϱ_{cb}, which is excited only in the presence of the coherent drive Ω_c.

To get some insight, we next discuss the weak plasmon field regime, where analytical solutions can be obtained. In the presence of a weak plasmon field, the populations ϱ_{cc}, ϱ_{aa} and the coherence ϱ_{ca} decouple from other equations. Using the initial conditions where $\varrho_{cc}(0)$, $\varrho_{cc}(0)$, $\varrho_{ac}(0)$ are non-zero, the drive field Ω_c is resonant with the transition $|a\rangle \leftrightarrow |c\rangle$, and the decay of the spasing transition is much faster than the drive transition $\gamma_b \gg \gamma_c$ one can obtain approximate analytical solutions as

$$\begin{aligned}\varrho_{aa}(t) = {}& \frac{e^{-\gamma_b t/2}}{16\Omega_c^2}\{4\Omega_c[-\gamma_b\sigma_{ac}(0) + 2(\varrho_{aa}(0) + \varrho_{cc}(0))\Omega_c] \\ & + [-\gamma_b^2\varrho_{aa}(0) + 4\gamma_b\sigma_{ac}(0)\Omega_c \\ & + 8(\varrho_{aa}(0) - \varrho_{cc}(0))\Omega_c^2]\cos 2\Omega_c t \\ & + 4\Omega_c[-\gamma_b\varrho_{aa}(0) + 4\sigma_{ac}(0)\Omega_c]\sin 2\Omega_c t\},\end{aligned} \tag{20}$$

$$\begin{aligned}\varrho_{cc}(t) = {}& \frac{e^{-\gamma_b t/2}}{16\Omega_c^2}\{4\Omega_c[-\gamma_b\sigma_{ac}(0) + 2(\varrho_{aa}(0) + \varrho_{cc}(0))\Omega_c] \\ & + [-\gamma_b^2\varrho_{aa}(0) + 4\gamma_b\sigma_{ac}(0)\Omega_c \\ & - 8(\varrho_{aa}(0) - \varrho_{cc}(0))\Omega_c^2]\cos 2\Omega_c t - 4\Omega_c \\ & \times [-\gamma_b\varrho_{aa}(0) + 4\sigma_{ac}(0)\Omega_c]\sin 2\Omega_c t\},\end{aligned} \tag{21}$$

$$\varrho_{ac}(t) = \mathrm{i}\frac{\mathrm{e}^{-\gamma_b t/2}}{16\Omega_c^2}\{\gamma_b[-\gamma_b\sigma_{ac}(0) + 2(\varrho_{aa}(0) + \varrho_{cc}(0))\Omega_c] - 2\Omega_c[\gamma_b(\varrho_{aa}(0) + \varrho_{cc}(0)) - 8\sigma_{ac}(0)\Omega_c\cos 2\Omega_c t - 8\Omega_c^2 \times [\varrho_{aa}(0) - \varrho_{cc}(0)]\sin 2\Omega_c t\}. \tag{22}$$

Generally the gain medium is pumped incoherently to transfer the quantum emitters from the ground state to excited states without generating any coherence. Without loss of any generality, we assume that the quantum emitters are incoherently excited to the state $|c\rangle$, i.e. $\varrho_{cc}(0) = 1$, $\varrho_{cc}(0) = \varrho_{ac}(0) = 0$. With these initial conditions, equations (20)–(22) take a simpler form, as

$$\varrho_{aa}(t) = \mathrm{e}^{-\gamma_b t/2}\sin^2\Omega_c t, \tag{23}$$

$$\varrho_{cc}(t) = \mathrm{e}^{-\gamma_b t/2}\left[\cos^2\Omega_c t + \frac{\gamma_b}{4\Omega_c}\sin 2\Omega_c t\right], \tag{24}$$

$$\varrho_{ac}(t) = \mathrm{i}\frac{\mathrm{e}^{-\gamma_b t/2}}{2}\left[\frac{\gamma_b}{2\Omega_c}\sin^2\Omega_c t + \sin 2\Omega_c t\right]. \tag{25}$$

Furthermore, the population inversion on the transition $|a\rangle \rightarrow |b\rangle$, defined as $n_{ab} = \varrho_{aa} - \varrho_{bb}$, can be obtained as

$$n_{ab}(t) = -1 + \frac{\mathrm{e}^{-\gamma_b t/2}}{2}\left[3 - \left(\cos 2\Omega_c t - \frac{\gamma_b}{2\Omega_c}\sin 2\Omega_c t\right)\right]. \tag{26}$$

Both, the drive field and the decay rates determine the strength of oscillations in the temporal evolution of population inversion. From equations (5) and (6) we obtain the evolution of the coherent ϱ_{ab} as

$$\ddot{\varrho}_{ab} + \Gamma_{ab}\dot{\varrho}_{ab} + |\Omega_c|^2\varrho_{ab} - \Omega_c\Omega\alpha_n\varrho_{ca} = 0. \tag{27}$$

In the weak plasmon field limit, the solution of this equation is of the form $\varrho_{ab} = \mathrm{i}\Omega\alpha_n\sigma_{ab}$ and the temporal evolution of LSP can be written as

$$\int_{\alpha_n(0)}^{\alpha_n(t)}\frac{\mathrm{d}\alpha_n}{\alpha_n} = -\int_0^t\{\Gamma_n + \mathcal{N}|\Omega|^2\sigma_{ab}(t')\}\mathrm{d}t'. \tag{28}$$

Performing the integration yields

$$\alpha_n(t) = \alpha_n(0)\mathcal{G}(t)\mathrm{e}^{-\Gamma_n t} \tag{29}$$

where $\mathcal{G}(t)$ is the integrated gain, defined as $\mathcal{G}(t) = \mathrm{e}^{-\mathcal{N}|\Omega|^2\int_0^t\sigma_{ab}(t')\mathrm{d}t'}$. From equation (29) we see that the integrated gain has to exceed the plasmonic loss to achieve amplification and eventually lasing of the SPs. In figure 4 we plot the integrated localized surface plasmons ($\mathcal{N}_{\mathrm{LSP}}^{\mathrm{Int}}$) versus the strength of the coherent drive field Ω_a (solid curve) and incoherent pump rate $\mathcal{R}$ (dashed curve). Here the results for incoherent pump is scaled by 50-fold. The effect of coherent drive field is two-fold. First, the magnitude of the total LSP generated significantly increases; and second, two-fold reduction in the threshold for achieving spasing.

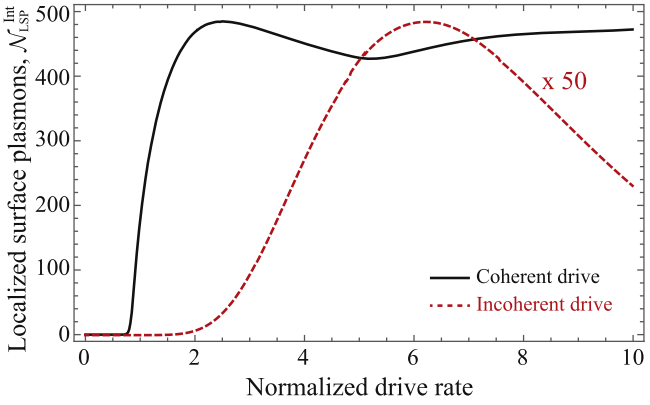

Figure 4. Plot of the integrated localized surface plasmons ($\mathcal{N}_{\mathrm{LSP}}^{\mathrm{Int}}$) versus the strength of the coherent drive field Ω_c(solid curve) and incoherent pump rate $\mathcal{R}$ (dashed curve). Here the results for incoherent pump is scaled by 50-fold. The effect of coherent drive field is two-fold. First, the magnitude of the total LSP generated significantly increases; and second, two-fold reduction in the threshold for achieving spasing. The number density of the quantum emitter is $\mathcal{N} = 1.25 \times 10^{21}\,\mathrm{cm}^{-3}$.

In this paper, we have focused on surface plasmon amplification by stimulated by emission of radiation in the transient regime, when population inversion is difficult to achieve due to fast relaxation rates, impractical pumping requirements, etc. We show that quantum coherence induced by the coherent drive field plays a crucial role in controlling the dynamics of energy exchange between the gain medium and the (dipolar) localized surface plasmon mode of a silver nanosphere. In particular, under optimal conditions, we achieved two orders of magnitude enhancement in LSP generation when the upper transition ($|a\rangle \leftrightarrow |c\rangle$) of the quantum emitter is driven coherently rather than pumped incoherently. Furthermore, with coherent excitation, we showed that quantum coherence and interference effects enables stronger emission of LSPs without population inversion on the spasing transition. Extending the domain of quantum coherence beyond its conventional platform of atomic, molecular and optical physics could lead to new horizons in ultrafast and controllable nanoplasmonics devices [50–52] for quantum optical applications, down to the single plasmon level.

Acknowledgements

The design and theoretical modeling of this work is supported by the Office of Naval Research (ONR) MURI program under Grant No. N00014-13-1-0649; the numerical calculation is supported by the 'Light-Material Interactions in Energy Conversion' Energy Frontier Research Center funded by the U.S. Department of Energy, Office of Science, Office of Basic Energy Sciences under Award Number DE-AC02-05CH11231.

References

[1] Weiner J and Nunes F 2013 *Light-Matter Interaction: Physics and Engineering at the Nanoscale* (Oxford: Oxford University Press)
[2] Zagoskin A M 2011 *Quantum Engineering: Theory and Design of Quantum Coherent Structures* (Cambridge: Cambridge University Press)
[3] Lienau C, Noginov M A and Loncar M 2014 *J. Opt.* **16** 110211
[4] Anker J N, Hall W P, Lyandres O, Shah N C, Zhao J and Duyne R P V 2008 *Nature Mater.* **7** 442
[5] Kim S, Jin J H, Kim Y J, Park I Y, Kim Y and Kim S W 2008 *Nature* **453** 757
[6] Voronine D V, Sinyukov A M, Hua X, Wang K, Jha P K, Munusamy E, Wheeler S E, Welch G R, Sokolov A V and Scully M O 2012 *Sci. Rep.* **2** 891
[7] Sharma B, Frontiera R R, Henry A, Ringe E and van Duyne R P 2012 *Mater. Today* **15** 16
[8] Stockman M I 2011 *Phys. Today* **64** 39
[9] Stockman M I 2011 *Opt. Exp.* **19** 22029
[10] Bergman D J and Stockman M I 2003 *Phys. Rev. Lett.* **90** 027402
[11] Noginov M A, Zhu G, Belgrave A M, Bakker R, Shalaev V M, Narimanov E E, Stout S, Herz E, Suteewong T and Wiesner U 2009 *Nature* **460** 1110
[12] Oulton R F, Sorger V J, Zentgraf T, Ma R-M, Gladden C, Dai L, Bartal G and Zhang X 2009 *Nature* **461** 629
[13] Chang D E, Sorensen A S, Hemmer P R and Lukin M D 2006 *Phys. Rev. Lett.* **97** 053002
[14] Lawandy L M 2004 *Appl. Phys. Lett.* **85** 5040
[15] Seidel J, Grafstroem S and Eng L 2005 *Phys. Rev. Lett.* **94** 177401
[16] Stockman M I 2008 *Nat. Photonics* **2** 327
[17] Ambati M, Nam S H, Ulin-Avila E, Genov D A, Bartal G and Zhang X 2008 *Nano Lett.* **8** 3998
[18] Ambati M, Genov D A, Oulton R F and Zhang X 2008 *IEEE J. Sel. Top. Quantum Electron.* **14** 1395
[19] Stockman M I 2010 *J. Opt.* **12** 024004
[20] Hess O and Tsakmakidis K L 2013 *Science* **339** 654–5
[21] Hess O, Pendry J B, Maier S A, Oulton R F, Hamm J M and Tsakmakidis K L 2012 *Nat. Mater.* **11** 573–84
[22] Wuestner S, Pusch A, Tsakmakidis K L, Hamm J M and Hess O 2010 *Phys. Rev. Lett.* **105** 127401
[23] Martikainen J-P, Hakala T K, Rekola H T and Torma P 2016 *J. Opt.* **18** 024006
[24] Khurgin J B and Sun G 2012 *Appl. Phys. Lett.* **100** 011105
[25] Khurgin J B and Sun G 2012 *Nanophotonics* **1** 3
[26] Khurgin J B 2015 *Nat. Nanotechnol.* **10** 2
[27] Boller K J, Imamoglu A and Harris S E 1991 *Phys. Rev. Lett.* **66** 2593
[28] Field J E, Hahn K H and Harris S E 1991 *Phys. Rev. Lett.* **67** 3062
[29] Kocharovskaya O 1992 *Phys. Rep.* **219** 175
[30] Kash M M, Sautenkov V A, Zibrov A S, Hollberg L, Welch G R, Lukin M D, Rostovtsev Y, Fry E S and Scully M O 1999 *Phys. Rev. Lett.* **82** 5229
[31] Budker D, Kimball D F, Rochester S M and Yashchuk V V 1999 *Phys. Rev. Lett.* **83** 1767
[32] Fleischhauer M and Scully M O 1994 *Phys. Rev.* A **49** 1973
[33] Jain M, Field J E and Yin G Y 1993 *Opt. Lett.* **18** 998
[34] Jain M, Xia H, Yin G Y, Merriam A J and Harris S E 1996 *Phys. Rev. Lett.* **77** 4326
[35] Jha P K, Mrejen M, Kim J, Wu C, Wang Y, Rostovtsev Y V and Zhang X 2016 *Phys. Rev. Lett.* **116** 165502
[36] Engel G S, Calhoun T R, Read E L, Ahn T K, Mancal T, Cheng Y C, Blankenship R E and Fleming G R 2007 *Nature* **446** 782
[37] Collini E, Wong C Y, Wilk K E, Curmi P M, Brumer P and Scholes G D 2010 *Nature* **463** 644
[38] Dorfman K E, Jha P K and Das S 2011 *Phys. Rev.* A **84** 053803
[39] Jha P K, Ni X, Wu C, Wang Y and Zhang X 2015 *Phys. Rev. Lett.* **115** 025501
[40] Dorfman K E, Jha P K, Voronine D V, Genevet P, Capasso F and Scully M O 2013 *Phys. Rev. Lett.* **111** 043601
[41] Jha P K, Yin X and Zhang X 2013 *Appl. Phys. Lett.* **102** 091111
[42] Voronine D V, Huo W and Scully M 2014 *J. Opt.* **16** 114013
[43] Kilin S Y, Kapale K T and Scully M O 2008 *Phys. Rev. Lett.* **100** 173601
[44] Sete E A, Svidzinsky A A, Rostovtsev Y V, Eleuch H, Jha P K, Suckewer S and Scully M O 2012 *IEEE J. Sel. Top. Quantum Electron.* **18** 541
[45] Jha P K, Svidzinsky A A and Scully M O 2012 *Laser Phys. Lett.* **9** 368
[46] Jha P K 2013 *Coherent Opt. Phenom* **1** 25
[47] Kolwas K and Derkachova A 2010 *Opto-Electron. Rev.* **18** 429
[48] Harris S E and Macklin J J 1989 *Phys. Rev.* A **40** 4135
[49] Scully M O and Zubairy M S 1997 *Quantum Optics* (Cambridge: Cambridge University Press)
[50] Jha P K, Mrejen M, Kim J, Wu C, Yin X, Wang Y and Zhang X 2014 *Appl. Phys. Lett.* **105** 111109
[51] Jacob Z and Shalaev V M 2011 *Science* **334** 463
[52] Tame M S, McEnery K R, Ozdemir S K, Lee J, Maier S A and Kim M S 2013 *Nature Phys.* **9** 329